Linking ITCZ migrations to AMOC and North Atlantic/Pacific SST decadal variability

E. Moreno-Chamarro [1,2,*], J. Marshall [1], and T. L. Delworth [3]

1. Department of Earth, Atmospheric, and Planetary Sciences. Massachusetts Institute of Technology, Cambridge, MA, USA.
2. Present address: Barcelona Supercomputing Center (BSC), Barcelona, Spain.
3. NOAA/Geophysical Fluid Dynamics Laboratory, Princeton, NJ, USA
* Corresponding author: eduardo.moreno@bsc.es

Abstract

We examine the link between migrations in the Intertropical Convergence Zone (ITCZ) and changes in the Atlantic meridional overturning circulation (AMOC), the Atlantic Multidecadal Variability (AMV), and the Pacific Decadal Oscillation (PDO). We focus on variations in interhemispheric heat transport in a coupled climate model which allows us to integrate over climate noise and assess underlying mechanisms. We use an ensemble of 10 simulations forced by a 50-year oscillatory NAO-derived surface heat flux anomaly in the North Atlantic, and a 4000-year-long preindustrial control simulation performed with the GFDL's CM2.1 climate model. In both setups, an AMV phase change induced by a change in the AMOC's cross-equatorial heat transport forces an atmospheric interhemispheric energy imbalance which is compensated by a change in the cross-equatorial atmospheric heat transport due to a meridional ITCZ shift. Such linkages occur on decadal timescales in the ensemble driven by the imposed forcing, and internally on multicentennial timescales in the control. Regional precipitation anomalies differ between the ensemble and the control for a zonally averaged ITCZ shift of similar magnitude, which suggests a dependence on timescale. Our study supports observational evidence of an AMV–ITCZ link in the 20th century and further extends it to the AMOC, whose long-timescale variability can influence the phasing of ITCZ migrations. In contrast to the AMV, our calculations suggest that the PDO does not drive ITCZ migrations, because the PDO does not

modulate the interhemispheric energy balance.

1. Introduction

The strong moisture convergence in the lower branch of the Hadley circulation sets the position of the Intertropical Convergence Zone (ITCZ), a narrow band of intense precipitation that encircles the Earth near the Equator. The meridional position of the zonally averaged Hadley circulation and ITCZ is tied to the atmospheric energy balance between the Northern and Southern hemispheres (NH and SH respectively) [e.g., Chiang and Friedman, 2012; Schneider et al., 2014]. In the present-day climate the NH is heated more strongly than the SH in the annual mean [as described in Frierson et al., 2013, Marshall et al, 2014]. To compensate for this imbalance, the Hadley circulation—the main driver of meridional energy transport in the tropics—and the ITCZ are located north of the Equator, thus allowing a net southward atmospheric energy transport across the Equator. Similarly, over the seasonal cycle the Hadley circulation and the ITCZ migrate meridionally following the solar-driven heating imbalance, transporting energy into the colder, winter hemisphere [e.g., Donohoe et al., 2013]. On longer timescales, a variety of modelling studies have shown that the Hadley cells shift meridionally as a result of atmospheric heating imbalances driven by changes in the Atlantic Ocean heat transport [Vellinga and Wu, 2004; Zhang and Delworth, 2005; Broccoli et al., 2006; Sun et al., 2013; Frierson et al, 2013; Marshall et al, 2014] or Arctic ice cover [Chiang and Bitz, 2005], as well as in future global warming scenarios [Frierson and Hwang, 2012]. Paleoclimate proxy records also suggest that strong NH cooling was linked to a southward shift of the Hadley circulation and ITCZ during Heinrich and Dansgaard-Oeschger events [e.g., Chiang and Friedman, 2012; McGee et al., 2018]. In observations over the 20th century, the ITCZ position appears connected to interhemispheric heating imbalance driven by multidecadal variability in the extratropical sea-surface temperature (SST) of the North Atlantic (Atlantic Multidecadal Variability, AMV) [Green et al., 2017]. Yet, whether this link can ultimately be extended to AMOC multidecadal variability is difficult to answer with the inadequate observational record. Moreover, observational estimates disagree on the influence of the North Pacific SST multidecadal variability (Pacific Decadal Oscillation, PDO) on ITCZ position [Green et al., 2017] and the potential linking mechanisms. Therefore, here we use a climate model to explore the connection between the AMOC, the North Pacific and Atlantic SST variability characterized by the AMV and PDO, and the ITCZ meridional position.

The AMV is a same-signed, basin-scale, multidecadal fluctuation of the North Atlantic SST that has been observed in the 20th century superimposed to the long-term warming trend [Kerr et al., 2000]. Phase changes of the AMV impact global tropical precipitation, especially in the West African and East Asian monsoon regions as well as the ITCZ meridional position [e.g., Folland et al., 2001; Zhang and Delworth, 2006; Mohino et al., 2011; Rupich-Robert et al., 2016]. ITCZ migrations have been connected to the interhemispheric heating contrast associated with North Atlantic SST anomalies, which warm or cool the entire NH troposphere with respect to the SH [e.g., Green et al., 2017]. Since the AMV has a causal link to multidecadal variability in the AMOC's northward heat transport [as reviewed in Buckley and Marshall, 2016], multidecadal AMOC and ITCZ variability might, by extension, also be linked, which offers a window for improved predictability of ITCZ migrations via AMOC predictability [Tulloch and Marshall, 2012].

The PDO is a multidecadal fluctuation of the tropical and mid-latitude North Pacific SSTs that presents colder central North Pacific SSTs and warmer SSTs along the American west coast during its positive phase, and vice versa [Mantua et al., 1997]. The PDO has been attributed to mid-latitude ocean–atmosphere feedbacks relating the Aleutian Low and surface winds over the North Pacific [as reviewed in Liu, 2012 and Newman et al., 2016]. Although the PDO has been connected to tropical precipitation changes over Central America, northern South America, western Australia, South India, and Central Africa [Mantua and Hare, 2002], it is poorly correlated with ITCZ shifts over the 20th century [Green et al., 2017]. Perhaps, this is because interhemispheric heating differences are unlikely to arise from changes in the Pacific Ocean heat transport, which is smaller than in the Atlantic [Trenberth and Caron, 2001] and characterized by shallow wind-driven meridional circulation cells [Ferrari and Ferreira, 2011]. The ITCZ–PDO connection seems thus rather tenuous, at least as revealed by the current observational record.

Better understanding the potential connections between variability of the AMOC, AMV, PDO, and ITCZ is of key importance, given the huge impacts of tropical precipitation distribution on the billions of people who live in the tropics. In this study, therefore, we explore links between AMV, AMOC, and PDO with ITCZ position, and whether they are robust in time and across timescales in a climate model following two different experimental setups, which present different AMV characteristics. Our analysis will help assess and validate the most recent conclusions drawn from observations over the 20th century. The structure of the paper is as follows: the model and experimental setup are described in Section 2. Section 3 documents the main results of the climate model simulations. A discussion of the key results and the main conclusions follow in Sections 4 and 5 respectively.

2. Model description and experimental setup

We use the GFDL CM2.1 climate model, which consists of atmosphere, ocean, land, and sea ice components. The atmospheric model has a 2.5x2 horizontal resolution and 24 vertical levels. The ocean model has a nominal horizontal resolution of 1° in the extra-tropics, with the meridional grid-spacing in the tropics gradually decreasing to a minimum of 1/3° near the Equator, and 50 vertical levels, with 22 evenly spaced levels in the top 220 m. The model does not use flux adjustments. A more detailed description of the model is given in Delworth et al. [2006]. This model has been used in a variety of studies of climate variability, predictability, and change, and an extensive model output from previous studies is available at https://nomads.gfdl.noaa.gov/CM2.X/.

Our analysis is based on two types of simulations with the same model. We first use a 300-year-long ensemble of 10 members which are forced by a surface heat flux anomaly derived from regressing reanalysis ocean–atmosphere heat flux anomalies onto the winter NAO index [Delworth and Zeng, 2016]. The forcing is added as an additional flux component to the normally computed air–sea heat flux, but only in the Atlantic sector, from the Equator to 82°N, including the Barents and Nordic seas. The forcing anomaly is computed ensuring its areal-integral is zero, and so does not provide a net heating or cooling to the climate system. The amplitude of the added NAO heat flux is modulated sinusoidally in time with a single period of 50 years and an amplitude of one standard deviation. For a more detailed description of how these simulations were designed we refer to Delworth and Zeng [2012]. We second use a 4000-year-long preindustrial control simulation in which all forcings are kept constant at 1860 conditions. In contrast to the ensemble, this calculation simulates a long control climate with unforced, internal variability. It is also described in detail in Delworth and Zeng [2012].

We define indices for the ITCZ position, AMV, AMOC strength, interhemispheric temperature difference, and PDO. The ITCZ position (Pcent) is defined as the latitude that divides regions of equal zonally averaged, annual mean total precipitation between 20°S and 20°N (i.e., the centroid), as in Donohoe et al. [2013]. The AMV index is the difference between the average North Atlantic SST and the global SST in the annual mean, following Trenberth and Shea [2006]. The AMOC strength is calculated as the annual mean overturning circulation averaged between 35°N and 45°N at 1000 m depth (corresponding to the position of the climatological maximum of the overturning cell; not shown). The inter-hemispheric temperature contrast is the difference between the NH and SH annual mean atmospheric temperature averaged between the surface and 300 hPa. The PDO index is the first principal component of the annual mean SST over the North Pacific Ocean between 20°N and 70°N [Mantua et al., 1997; Newman et al., 2016].

We compare composites that include years that are more than one standard deviation above and below the long-term mean of each index. Statistical significance of the anomalies between these two composites is calculated based on the likelihood of a random occurrence of the signal: the signals detected are compared to analogs obtained by, first, randomly sampling each index 1000 times and, then, repeating the same analysis; we use the 5th and 95th percentiles of the empirical anomaly distribution to set the confidence levels.

3. Analysis of the model simulations

i) Forced ensemble

The link between the ITCZ, AMV, and AMOC is first explored in the 10-member ensemble mean. We focus on the ensemble-mean since this helps increase the signal-to-noise ratio and so allows one to more readily characterize the forced variability. In the ensemble mean, Pcent, AMV, AMOC strength, and interhemispheric temperature difference all exhibit 50-year periodicity following that of the imposed forcing (Fig. 1). There is strong covariability between the four indices on multidecadal timescales in the second half of the 300-year-long simulated period (red shading in Supp. Fig. 1). Furthermore, AMOC variability leads the other three indices, while the AMV and temperature difference vary in phase and lead Pcent ITCZ variability (arrows in Supp. Fig. 1, and Supp. Fig. 2).

Precipitation anomaly patterns following a phase change of the AMOC and AMV are broadly similar and reflect an ITCZ shift (Fig. 2b,c). A strong AMOC and a warm AMV lead to a precipitation increase in most of the NH tropics, especially in the tropical North Atlantic and North Pacific and Sahel, and a precipitation decrease most notably in Southeastern Asia, the tropical South Pacific, Brazil, and the equatorial Atlantic. Such precipitation changes are further associated with an overall strengthening and weakening of the trade winds in the SH and NH, respectively (arrows in Fig. 2), related to a northward shift of the Hadley circulation. Precipitation anomalies driven by the AMOC and AMV are similar to those of an ITCZ shift, although anomalies in the latter case are larger and more widespread in the Northwestern and Central tropical Pacific and less so in the tropical Atlantic, Sahel, and South America. Regional mechanisms, such as the Bjerkness feedback (by which initial SST anomalies get amplified as they weaken the trade winds aloft) [Bjerkness, 1969], might explain these differences, because a positive AMV phase would especially favor atmospheric convection in the tropical Atlantic.

Despite these differences, both a warm AMV and a strong AMOC lead to a northward shift of the ITCZ and Hadley circulation of similar magnitude and shape in the zonal average (Fig. 2, right panels).

Periodicity in the Pcent, AMV, AMOC, and interhemispheric temperature difference results from the change in buoyancy flux forced by the oscillatory heat flux anomaly, especially over the Labrador Sea surface: for a negative downward heat flux anomaly, upper-ocean cooling enhances ocean deep mixing, which strengthens the AMOC and its associated poleward heat transport. This warms the North Atlantic surface (warm AMV phase) in the following 5 to 10 years. Upper-ocean warming propagates to the troposphere aloft, where it gets quickly distributed to all longitudes and vertically by the atmospheric circulation, which results in a NH troposphere, which is warmer than in the SH (as indicated by a positive interhemispheric temperature difference). This is well illustrated in Figs. 3 and 4 by the close correspondence between the anomaly patterns of the asymmetric component of the zonally averaged tropospheric temperature and the Atlantic oceanic heat transport (OHT). The ITCZ and the Hadley circulation move northward to compensate for a warmer NH, thus permitting southward cross-equatorial atmospheric heat transport (AHT; Fig. 4). The OHT in the Pacific and Indian oceans (Fig. 4) also contributes to this compensation by transporting heat southward across the Equator as a result of the change in the wind-driven oceanic subtropical cells [Green and Marshall, 2017].

The PDO shows synchronous coherence with the Pcent and lags behind changes in the AMV and the interhemispheric temperature difference between years 150–300 on the timescales of the applied forcing (see Supplementary Material). This suggests that a positive PDO tends to develop after a positive AMV phase warms the NH and shifts the ITCZ northward (and vice versa). The PDO time series, however, shows no evident 50-year cycle imposed by the surface heat forcing but centennial oscillations between a positive phase and a negative phase. Correlation coefficients between the PDO and the AMV are small and statistically non-significant at all lags. These results are different from those reported by Ruprich-Robert et al. [2016] in which a negative PDO develops after a warm AMV (and vice versa) in simulations with the same climate model (CM2.1) in which SSTs are restored to AMV anomalies. This might be caused by a larger amplitude in the tropical North Atlantic SSTs in the case when they are restored than in our case, when they are induced by AMOC variations, resulting in a stronger teleconnection between the Atlantic and the Pacific tropical atmosphere.

The patterns of anomalies shown in Figures 2, 3 and 4 in net precipitation, zonally-averaged asymmetric temperature, and OHTs and AHT precede the PDO by a few years (Supp. Fig. 2) and are very similar to those related to an ITCZ/AMV shift. This reinforces our conclusion that, in our simulations, a PDO shift tends to follow one in the ITCZ and/or AMV. However, a PDO phase shift does not induce an interhemispheric heating anomaly or an ITCZ shift in subsequent years (Supp. Figs. 1 and 2). This discards the PDO as driver of variability in the meridional position of the ITCZ in our simulations.

ii) Control simulation

We extend our analysis to a 4000-year control simulation with preindustrial forcing performed with the same climate model. Here, synchronous coherence between AMOC and AMV variability, and between the latter and the interhemispheric temperature difference (indices in Fig. 5) extends over the 4000 years on multicentennial especially (Supp. Fig. 3). The spectrum of these three indices exhibits a strong peak centered at a period of about 250 years which is statistically significant at the 1% level (Supp. Fig. 4). Note that the AMV shows no relative maximum in its spectrum on a timescale of 50–70 years, a feature of observations [Frankcombe et al., 2010]. Our model results support the connection between a strong AMOC and a warming of the the North Atlantic surface and, by extension, of the entire NH. However, co-variability between the Pcent and AMV is less evident than in the forced simulations described above. This suggests that interhemispheric heating imbalances associated with an AMV phase shift tend to be compensated more effectively by a change in the top-of-the-atmosphere radiative balance or the ocean heat uptake, or both, than by a change in cross-equatorial AHT through an ITCZ shift. Nonetheless, Pcent, AMOC, and AMV variability show significant coherence on multi centennial timescales between years 500 and 2000 years, when the interhemispheric temperature difference shows some of the largest variations over the 4000 years of the control integration. However, there is non-significant coherence on decadal and multidecadal timescales between years 3000 and 4000 approximately, and in a 500-year-long period centred around year 3000 (Supp. Fig. 3). Over all these periods, Pcent lags behind changes in the AMOC and AMV by a few decades (arrows in Supp. Fig. 3). Coherence between Pcent and AMV or AMOC thus appears to be intermittent in time in the control. To focus on the most robust connection between the indices on multicentennial timescales, we apply a band-pass filter with a period range between 200 and 300 years to all the data (Supp. Fig. 5) and analyse the 1500-year-long period between years 500 and 2000.

The anomaly patterns of the band-passed precipitation related to a strong AMOC and a warm AMV are very similar to that for a northward ITCZ shift (Fig. 6). They show a wetter western tropical North and Central Pacific and North Atlantic and Sahel, and dryer Southeastern Asia, North Australia, Equatorial Central Pacific and Atlantic, and South America (Fig. 6). A northward ITCZ shift is also associated with NH warming anomalies (Supp. Fig. 7), driven by an anomalous AMOC's heat transport and warm North Atlantic surface (not shown), as in the ensemble mean calculation of the forced run described earlier. The timescale of the AMOC–AMV–ITCZ link are, however, longer in the control than in the forced simulations: a maximum northward ITCZ shift occurs about 24 years later than a maximum positive AMV in the control, but only 4 years later in the forced case (compare Supp. Figs. 6 and 2).

The PDO and the Pcent show out-of-phase co-variability only on multicentennial timescales, with a PDO warm phase during a southward ITCZ shift and vice versa (Supp. Fig. 3). Yet these two indices do not show any evident co-variability on centennial timescales in the period 500–2000 years, in contrast to AMV and Pcent (Supp. Fig. 3). Phase changes in the PDO are not clearly connected to an ITCZ shift in the control simulation (Fig. 6d) and are not associated with significant interhemispheric temperature differences (Supp. Fig. 7d). This reinforces our previous conclusions that the PDO–ITCZ connection is far less distinct than the AMV–ITCZ one .

4. Discussion

Both the 10-member ensemble mean and the control simulation show that the zonally averaged meridional position of the ITCZ is linked to the North Atlantic SST and, by extension, to AMOC variability. This linkage results from the interhemispheric atmospheric heating imbalance driven by a change in the Atlantic cross-equatorial OHT impacting North Atlantic

SSTs, which is compensated by a meridional shift in the Hadley circulation and the ITCZ to enhance the cross-equatorial AHT into the colder hemisphere. This chain of events, however, only operates if the heating imbalance is not fully compensated by an adjustment in the top-of-the-atmosphere radiative flux or the ocean heat uptake, or both. This might explain why the linkage is not always found on all timescales and over the whole period in the control. Even though simulated AMOC variability is also pronounced on 20-year timescales in the control (Supp. Fig. 4), it has a smaller impact on AMV and ITCZ variability than on multicentennial timescales (Supp. Figs. 3 and 4). On these very long timescales, changes in the surface albedo of sea ice and low-level cloudiness amplify AMOC-related SST variations, leading to larger, more global impacts on tropospheric temperatures [Delworth and Zeng, 2012]. Such amplification might be key to triggering ITCZ shifts on multicentennial timescales rather than on shorter ones. In the ensemble mean, on the other hand, the mechanism linking the AMOC, the AMV, and the ITCZ is not fully active during the first 150 years. This is suggestive of an adjustment period, which is perhaps somewhat different in each ensemble member, causing the signal to be averaged out in the ensemble mean. Each ensemble member starts from a different point in the control simulation, and thus has a random phasing of internal variability. It appears to take some time before the NAO-related surface heat flux forcing is able to "synch up" the variability in the differing ensemble members. Furthermore, the linkage between the AMV and the ITCZ might be related to the amplitude of the changes in the interhemispheric temperature differences: in the forced ensemble on multidecadal timescales they are almost as large as those in the control on multicentennial timescales. Regardless of timescales or period, we find the meridional position of the ITCZ to be tied to changes in the AMOC through the AMV in both types of simulations.

Our model results thus support and expand those from the observations covering the 20th century [Green et al., 2017].

Compared to observations, AMOC variations induced in the model result in relatively small SST variations in the North Atlantic (of an amplitude of about 0.4 K in observations [Ting et al., 2009] and about 0.2 K in the model, Fig. 1). Such relatively small variations might also explain the discontinuous connection between the AMOC, the AMV, and the ITCZ in the model. Perhaps SST changes in the North Atlantic are not large enough to trigger a long-lasting, global response in atmospheric temperature and tropical precipitation. A relatively muted response might also hamper detecting such connections in the observations [Green et al., 2017]. A similar linkage between AMOC, AMV, and ITCZ can be found in the paleo-record, where the amplitude of the changes and, thus, the signal-to-noise ratio is indeed much larger. For example, an AMOC collapse and strong NH cooling support evidence of a southward ITCZ shift during Heinrich events over the past glacial period [e.g., Lynch-Stieglitz, 2017; McGee et al, 2018]. Fig. 7 illustrates this link through anomalies in net precipitation and near-surface wind between the Heinrich Event 1 and the Last Glacial Maximum in the TraCE-21ka simulation, a transient simulation of the last 21,000 years [Liu et al., 2009]. In this simulation, an anomalous freshwater flux is applied to the North Atlantic Ocean to trigger an AMOC shutdown. The large NH cooling associated with the reduction in the Atlantic cross-equatorial OHT forces a response in the ITCZ and Hadley circulation, which shift southward to permit an increase in the northward cross-equatorial AHT and thus compensate for the strong interhemispheric heating imbalance. This mechanism is essentially the same as the one which we have identified as operating in the CM2.1 model used here.

Although the zonally-averaged precipitation anomalies of the strong AMOC, warm AMV, and northward ITCZ shift are relatively similar in the control simulation and the ensemble mean, the spatial pattern of precipitation anomalies differ between the two simulations (compare Figs. 2 and 6). Moreover, both patterns are in turn different from each climatological mean (contours in Figs. 2 and 6). It is however important to note that precipitation anomalies develop on different timescales: multidecadal ones in the ensemble mean, and multicentennial ones in the control. The regional pattern of the ITCZ shifts may thus depend on the the timescale, in agreement with the results in Roberts et al. [2017]. Precipitation anomalies in the CM2.1 climate model are also different from those found in models which simulate a transition from the Last Glacial Maximum to the Heinrich Stadial 1, as in the TraCE-21ka simulation performed with the CCM3 model shown in Fig. 7. This suggests that regional precipitation anomalies related to an ITCZ shift may also be model dependent.

In addition to the spatial pattern, the response time of the ITCZ to AMOC and AMV variations is also different in the control and the forced ensemble. In the control, the cross-equatorial AHT and the associated ITCZ shift take longer than in the forced ensemble to respond to the interhemispheric heating imbalance. This might be related to the time other processes, like a change in the top-of-the-atmosphere energy flux, takes to compensate for the interhemispheric heating imbalance without a shift in the cross-equatorial AHT and the ITCZ. We propose that, only when the interhemispheric heating imbalance is large enough for it not to be fully compensated by those other processes, does an anomalous cross-equatorial AHT and/or OHT (for example, through a change in the strength of the subtropical cells; Green and Marshall, 2017) get triggered. This then shifts the ITCZ and Hadley circulation meridionally, yet delayed with respect to the onset of the heating imbalance. Furthermore, changes in the climate due to AMV phase and ITCZ shift might alter (decreasing) the effectiveness of the other processes compensating for the heating imbalance (for example, by changing the albedo or water vapor content of the atmosphere), increasing the role of the cross-equatorial AHT in its compensation and, hence, shifting the ITCZ farther (even if the heating imbalance has already started to get dampened). This might explain why the ITCZ shifts peaks some years later later than the AMV and the interhemispheric temperature difference. We also note that, somehow, the lag between the AMV and ITCZ appears to be related to the timescale of the linkage by a factor of 10 (50-year timescale and 4-year lag in the ensemble mean, and 250-year timescale and 24-year lag in the control; Figs. 2 and 6). These connections and delay will require further investigation in the future.

5. Conclusions

We have investigated the linkage between variability of the tropical SST in the North Atlantic and North Pacific, characterized by the AMV and PDO, the AMOC, and the meridional position of the ITCZ in two sorts of simulations with the GFDL's CM2.1 climate model: an ensemble of 10 simulations forced with a 50-year-long oscillatory anomaly of the North Atlantic surface heat flux related to the NAO, and a 4000-year-long preindustrial (with 1860's forcing conditions) control simulation. Our results indicate that:

1. Both in the ensemble mean and the control, changes in the cross-equatorial OHT driven by the AMOC lead to changes in the North Atlantic SST that shift the AMV phase. This, in turn, forces an interhemispheric heating imbalance that is compensated by a meridional shift in the

Hadley circulation and the ITCZ meridional position connected to widespread, global changes in the tropical precipitation. This result provides a clear link between the AMOC, AMV, and ITCZ variability. This link operates on multidecadal timescales in the ensemble mean, related to the imposed surface heat flux, and mainly on multicentennial timescales in the control, with a shorter lag between the peaks in the AMV and ITCZ variability in the ensemble mean than in the control (4 and 24 years respectively). In addition, the pattern of tropical precipitation anomalies is different between the control and the forced ensemble for a similar zonally-averaged ITCZ shift, which suggests a dependance on the timescale. Our results thus offer support for an AMV–ITCZ link over the 20th century hinted at in observations and further show it is driven by AMOC variability.

2. In contrast to the AMV, the ensemble mean and the control show no ITCZ shift following a change in the PDO. This is consistent with point 1. in that the PDO has a negligible impact on oceanic and atmospheric cross-equatorial heat transport and on the atmospheric interhemispheric energy balance.

Figure captions:

Fig. 1: Times series in the 10-member ensemble mean. Section 2 details how each index is defined. Time series are shown linearly detrended. Thin and thick lines are the yearly values and the 11-year running mean respectively.

Fig. 2: *Left*: anomalies in the annual-mean precipitation rate (shading; in mm/day) and 1000-hPa wind (arrows; in m/s) between years above and below one standard deviation in the decadally

smoothed indices in Fig. 1. Anomalies are calculated with the AMV and the AMOC leading by 4 and 10 years respectively, and the PDO lagging behind by 4 years (values derived from the cross-correlation profiles in Supp. Fig. 2) and only in the second half of the ensemble mean (years 151–300), when the Pcent, the AMV, and the AMOC show statistically significant coherence (see text and Supp. Fig. 1). Light and dark blue lines are the 3 mm/day and 6 mm/day precipitation climatologies respectively. *Right*: Zonally averaged anomalies in precipitation (blue) and wind (red) from the panels on the left. Stippling (left) and gray shading (right) mask anomalies that are non-significant at the 5% level.

Fig. 3: As in Fig. 2 but for the asymmetric component of the zonally averaged atmospheric temperature (in K). The AMV and the AMOC lead the temperature anomalies by 1 and 5 years respectively, and the Pcent and PDO lag behind by 3 and 5 years respectively (values derived from the cross-correlation profiles in Supp. Fig. 2).

Fig. 4: As in Fig. 2 but for anomalies in the heat transport (in PW) in the atmosphere (AHT; black line), the global ocean (OHT; pink) north of 30°S, the Atlantic Ocean (ATL-OHT; blue), and the Indo-Pacific oceans (IP-OHT; red). Anomalies are calculated with the AMOC in phase, and the Pcent, the AMV, and the PDO lagging behind by 8, 3, and 10 years respectively. Gray shading masks anomalies that are non-significant at the 5% level.

Fig. 5: Time series in the 4000-year control as in Fig. 1. Thin and thick lines are the 11- and the 51-year running means respectively.

Fig. 6: As in Fig. 2 but for the band-passed indices in the 4000-year control (see text for details; indices shown in Supp. Fig. 5). Calculations are only between years 500 and 2000, when the Pcent, the AMV, and the AMOC show coherence on centennial time scales (Supp. Figs. 3 and 4).

Precipitation anomalies lag behind the AMV and the AMOC by 24 years (values derived from the cross-correlation profiles in Supp. Fig. 6). No lead or lag is applied to the PDO.

Fig. 7: (a) Anomalies in the annual-mean precipitation rate (shading; in mm/day) and near-surface (10 m) winds between the Last Glacial Maximum and the Heinrich Stadial 1 (averaged over the periods 20–21 kyrs and 15.5–16.5 kyrs respectively) in the TraCE-21ka simulation. Anomalies are computed to illustrate that the ITCZ is farther north during the LGM than during the HS1 and, thus, for a better comparison with Figs. 2 and 6. Note that the shading color scale of the ocean temperature is adapted for a better view of the values in the range ±2 K. No significances are shown since almost of the anomalies are statistically significant at the 5 % level (for a two-tailed Student's t test in which effective degrees of freedoms and serial autocorrelation are taken into account). **(b)** Zonally averaged anomalies in the precipitation rate (blue) and wind (red) from **(a)**. Adapted from McGee et al. [2018].

Acknowledgements:

E.M.-C. And J.M. acknowledge support from NOAA award NA16OAR4310177.

References:

- Bjerknes, J. (1969). Atmospheric teleconnections from the equatorial Pacific. Monthly weather review, 97(3), 163-172.

- Broccoli, A. J., K. A. Dahl, and R. J. Stouffer (2006), Response of the ITCZ to Northern Hemisphere cooling, *Geophysical Research Letters*, 33, L01702.

- Buckley, M., and J. Marshall (2016), Observations, inferences, and mechanisms of the Atlantic

Meridional Overturning Circulation: A review, *Review of Geophysics*, 54, 5–63

- Chiang, J. C. H., and A. R. Friedman (2012), Extratropical cooling, interhemispheric thermal gradients, and tropical climate change, *Annual Reviews of Earth and Planetary Sciences*, 40, 383–412.

- Chiang, J. C. H., and C. M. Bitz (2005), Influence of high latitude ice cover on the marine Intertropical Convergence Zone, *Climate Dynamics*, 25, 477–496.

- Delworth, T. L., Broccoli, A. J., Rosati, A., Stouffer, R. J., Balaji, V., Beesley, J. A., ... & Durachta, J. W. (2006). GFDL's CM2 global coupled climate models. Part I: Formulation and simulation characteristics, *Journal of Climate*, 19(5), 643–674.

- Delworth, T. L., & Zeng, F. (2012). Multicentennial variability of the Atlantic meridional overturning circulation and its climatic influence in a 4000 year simulation of the GFDL CM2.1 climate model, *Geophysical Research Letters*, 39(13).

- Delworth, T. L., & Zeng, F. (2016). The impact of the North Atlantic Oscillation on climate through its influence on the Atlantic meridional overturning circulation, *Journal of Climate*, 29(3), 941–962.

- Donohoe, A., J. Marshall, D. Ferreira, and D. McGee (2013), The relationship between ITCZ location and cross-equatorial atmospheric heat transport: From the seasonal cycle to the last glacial maximum, *Journal of Climate*, 26, 3597–3618.

- Ferrari, R., & Ferreira, D. (2011). What processes drive the ocean heat transport?, *Ocean Modelling*, 38(3–4), 171–186.

- Folland, C. K., Colman, A. W., Rowell, D. P., & Davey, M. K. (2001). Predictability of northeast Brazil rainfall and real-time forecast skill, 1987–98, *Journal of Climate*, 14(9), 1937–

1958.

- Frankcombe, L. M., Von Der Heydt, A., & Dijkstra, H. A. (2010). North Atlantic multidecadal climate variability: an investigation of dominant time scales and processes, *Journal of Climate*, 23(13), 3626–3638.

- Frierson, D. M. W., and Y.-T. Hwang (2012), Extratropical influence on ITCZ shifts in slab ocean simulations of global warming, *Journal of Climate*, 25(2), 720–733.

- Frierson, D. M., Hwang, Y. T., Fučkar, N. S., Seager, R., Kang, S. M., Donohoe, A., ... & Battisti, D. S. (2013). Contribution of ocean overturning circulation to tropical rainfall peak in the Northern Hemisphere, *Nature Geoscience*, 6(11), 940–944.

- Green, B., & Marshall, J. (2017). Coupling of trade winds with ocean circulation damps ITCZ shifts, *Journal of Climate*, 30(12), 4395–4411.

- Green, B., Marshall, J., & Donohoe, A. (2017). Twentieth century correlations between extratropical SST variability and ITCZ shifts, *Geophysical Research Letters*, 44(17), 9039-9047.

- Kerr, R. A. (2000), A North Atlantic climate pacemaker for the centuries, *Science*, 288(5473), 1984–1985, doi:10.1126/science.288.5473.1984.

- Liu, Z. (2012). Dynamics of interdecadal climate variability: A historical perspective. *Journal of Climate*, 25(6), 1963-1995.

- Liu, Z., Otto-Bliesner, B. L., He, F., Brady, E. C., Tomas, R., Clark, P. U., ... & Erickson, D. (2009). Transient simulation of last deglaciation with a new mechanism for Bølling-Allerød warming, *Science*, 325(5938), 310–314.

- Lynch-Stieglitz, J. (2017). The Atlantic meridional overturning circulation and abrupt climate change, *Annual Review of Marine Science*, 9, 83–104.

- Mantua, N. J., & Hare, S. R. (2002). The Pacific decadal oscillation, *Journal of Oceanography*, 58(1), 35–44.

- Mantua, N. J., S. R. Hare, Y. Zhang, J. M. Wallace, and R. C. Francis (1997), A Pacific interdecadal climate oscillation with impacts on salmon production, *Bulletin of the American Meteorological Society*, 78(6), 1069–1079.

- Marshall, J., Donohoe, A., Ferreira, D., and McGee, D. (2014): The ocean's role in setting the mean position of the Inter-Tropical Convergence Zone, Climate Dynamics, vol. 42, no. 7-8, pp. 1967-1979.

- McGee, D., A. Donohoe, J. Marshall and D. Ferreira (2014): Changes in ITCZ location and cross-equatorial heat transport at the Last Glacial Maximum, Heinrich Stadial 1, and the mid-Holocene. Earth and Planetary Science Letters, Volume 390, 69-79

- McGee, D., Moreno-Chamarro, E., Green, B., Marshall, J., Galbraith, E., & Bradtmiller, L. (2018). Hemispherically asymmetric trade wind changes as signatures of past ITCZ shifts, *Quaternary Science Reviews*, 180, 214–228.

- Mohino, E., Janicot, S., & Bader, J. (2011). Sahel rainfall and decadal to multi-decadal sea surface temperature variability, *Climate Dynamics*, 37(3–4), 419–440.

- Newman, M., Alexander, M. A., Ault, T. R., Cobb, K. M., Deser, C., Di Lorenzo, E., ... & Schneider, N. (2016). The Pacific decadal oscillation, revisited. Journal of Climate, 29(12), 4399–4427.

- Roberts, W. H., Valdes, P. J., & Singarayer, J. S. (2017). Can energy fluxes be used to interpret glacial/interglacial precipitation changes in the tropics?, *Geophysical Research Letters*, 44(12), 6373–6382.

- Ruprich-Robert, Y., Msadek, R., Castruccio, F., Yeager, S., Delworth, T., & Danabasoglu, G. (2017). Assessing the climate impacts of the observed Atlantic multidecadal variability using the GFDL CM2.1 and NCAR CESM1 global coupled models, *Journal of Climate*, 30(8), 2785–2810.

- Schneider, T., T. Bischoff, and G. H. Haug (2014), Migrations and dynamics of the intertropical convergence zone, *Nature*, 513, 45–53.

- Sun, C., J. Li, F.-F. Jin, and R. Ding (2013), Sea surface temperature inter-hemispheric dipole and its relation to tropical precipitation, *Environmental Research Letters*, 8(4).

- Ting, M., Kushnir, Y., Seager, R., & Li, C. (2009). Forced and internal twentieth-century SST trends in the North Atlantic. Journal of Climate, 22(6), 1469–1481.

- Trenberth, K. E., and D. J. Shea (2006), Atlantic hurricanes and natural variability in 2005, *Geophysical Research Letters*, 33, L12704, doi:10.1029/2006GL026894.

- Trenberth, K. E., & Caron, J. M. (2001). Estimates of meridional atmosphere and ocean heat transports, *Journal of Climate*, 14(16), 3433–3443.

- Tulloch, R., and J. Marshall (2012), Exploring mechanisms of variability and predictability of Atlantic meridional overturning circulation in two coupled climate models, *Journal of Climate*, 25(12), 4067–4080, doi:10.1175/JCLI-D-11-00460.1.

- Zhang, R., and T. L. Delworth (2005), Simulated tropical response to a substantial weakening of the Atlantic thermohaline circulation, *Journal of Climate*, 18(12), 1853–1860.

- Zhang, R., and T. L. Delworth (2006), Impact of Atlantic multidecadal oscillations on India/Sahel rainfall and Atlantic hurricanes, *Geophysical Research Letters*, 33, L17712, doi:10.1029/2006GL026267.

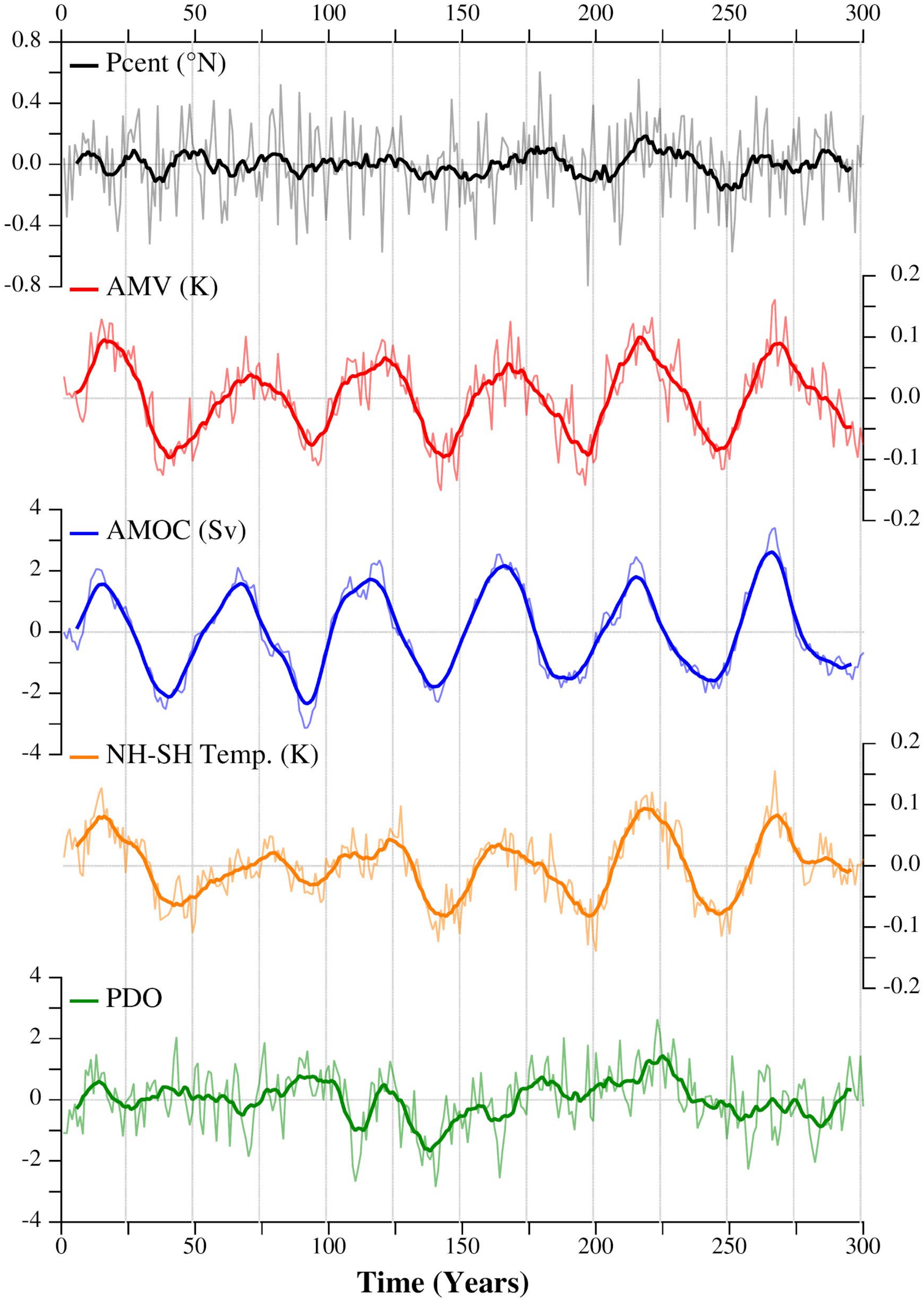

Fig. 1: Times series in the 10-member ensemble mean. Section 2 details how each index is defined. Time series are shown linearly detrended. Thin and thick lines are the yearly values and the 11-year running mean respectively.

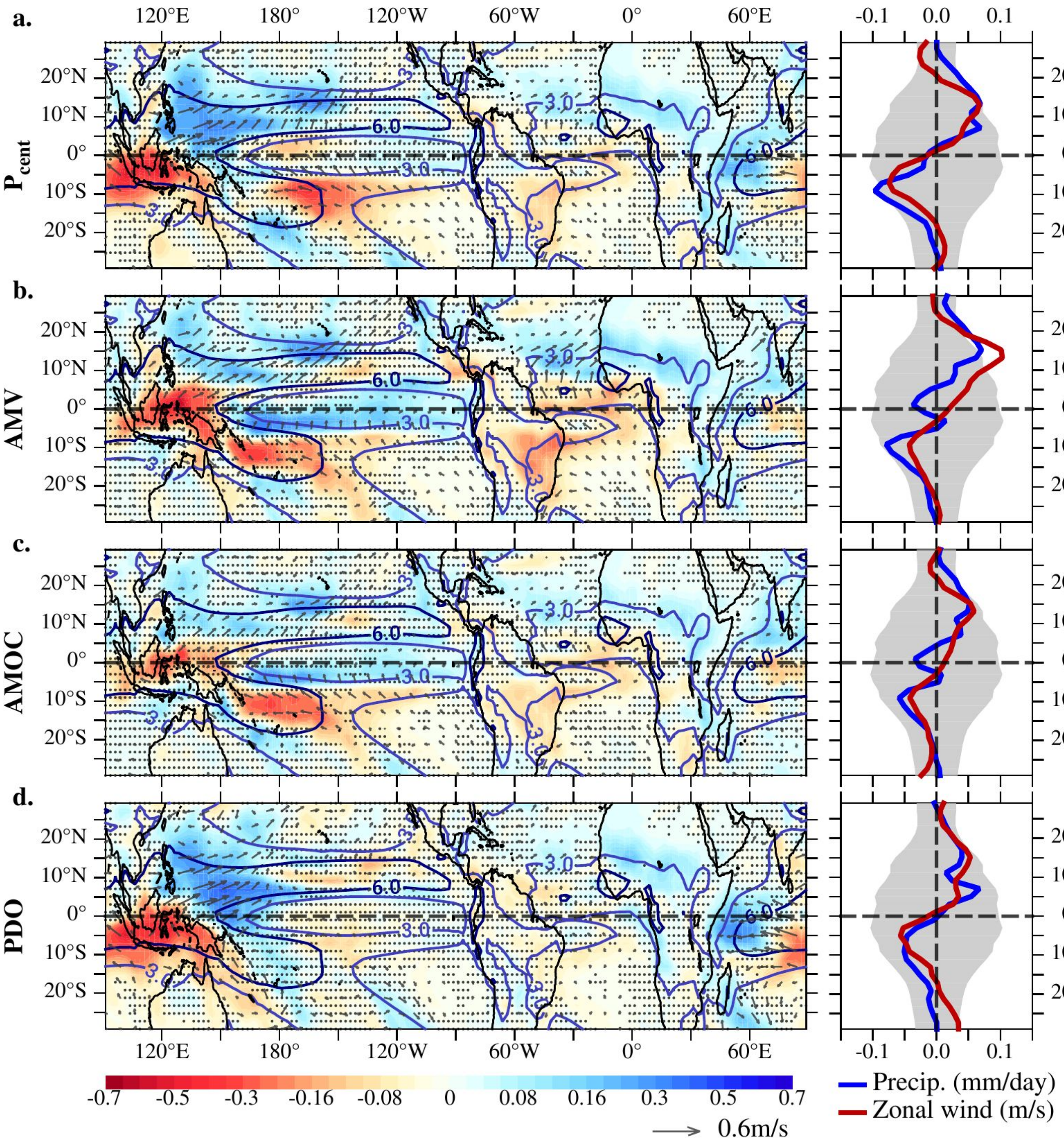

Fig. 2: *Left*: anomalies in the annual-mean precipitation rate (shading; in mm/day) and 1000-hPa wind (arrows; in m/s) between years above and below one standard deviation in the decadally smoothed indices in Fig. 1. Anomalies are calculated with the AMV and the AMOC leading by 4 and 10 years respectively, and the PDO lagging behind by 4 years (values derived from the cross-correlation profiles in Supp. Fig. 2) and only in the second half of the ensemble mean (years 151–300), when the Pcent, the AMV, and the AMOC show statistically significant coherence (see text and Supp. Fig. 1). Light and dark blue lines are the 3 mm/day and 6 mm/day precipitation climatologies respectively. *Right*: Zonally averaged anomalies in precipitation (blue) and wind (red) from the panels on the left. Stippling (left) and gray shading (right) mask anomalies that are non-significant at the 5% level.

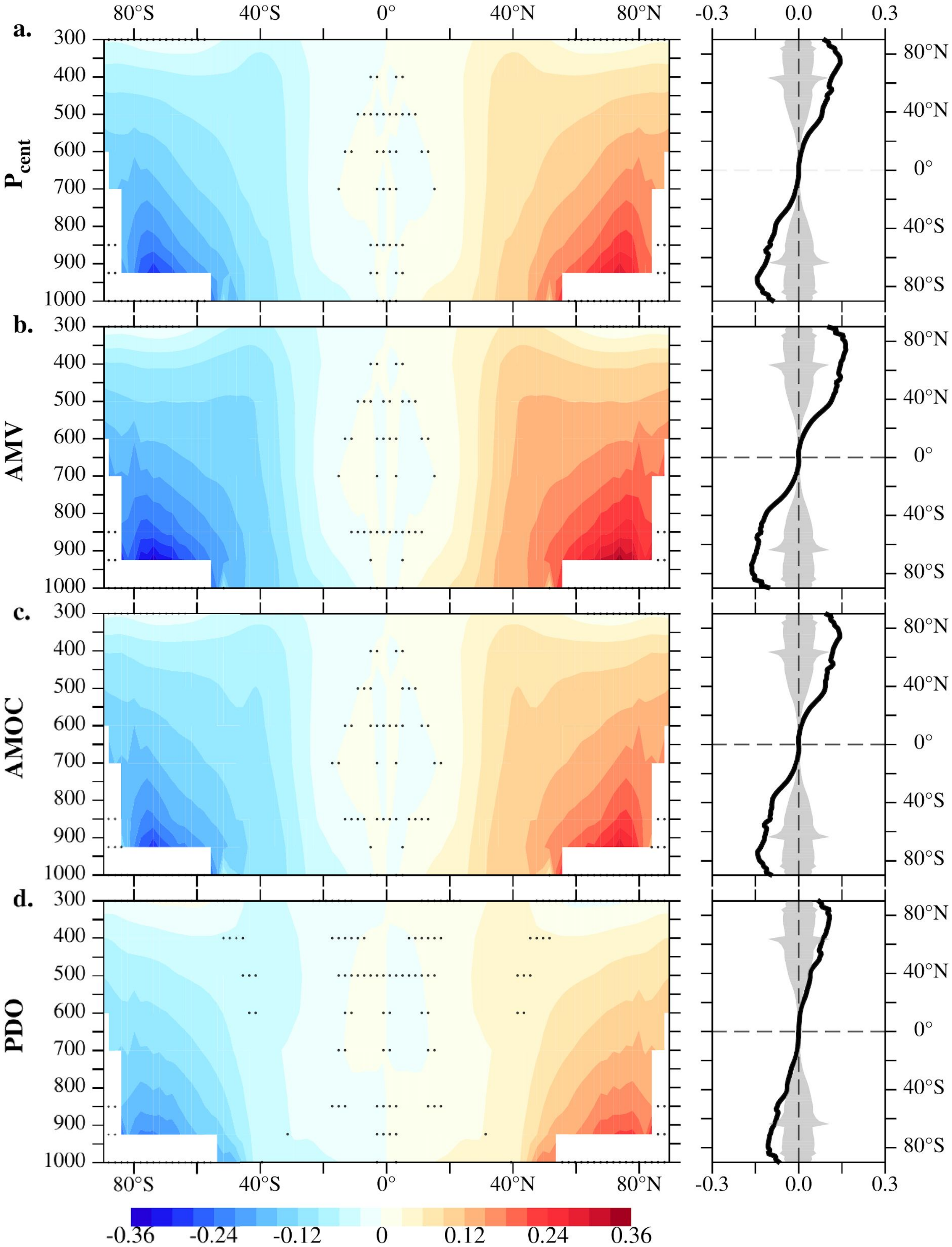

Fig. 3: As in Fig. 2 but for the asymmetric component of the zonally averaged atmospheric temperature (in K). The AMV and the AMOC lead the temperature anomalies by 1 and 5 years respectively, and the Pcent and PDO lag behind by 3 and 5 years respectively (values derived from the cross-correlation profiles in Supp. Fig. 2).

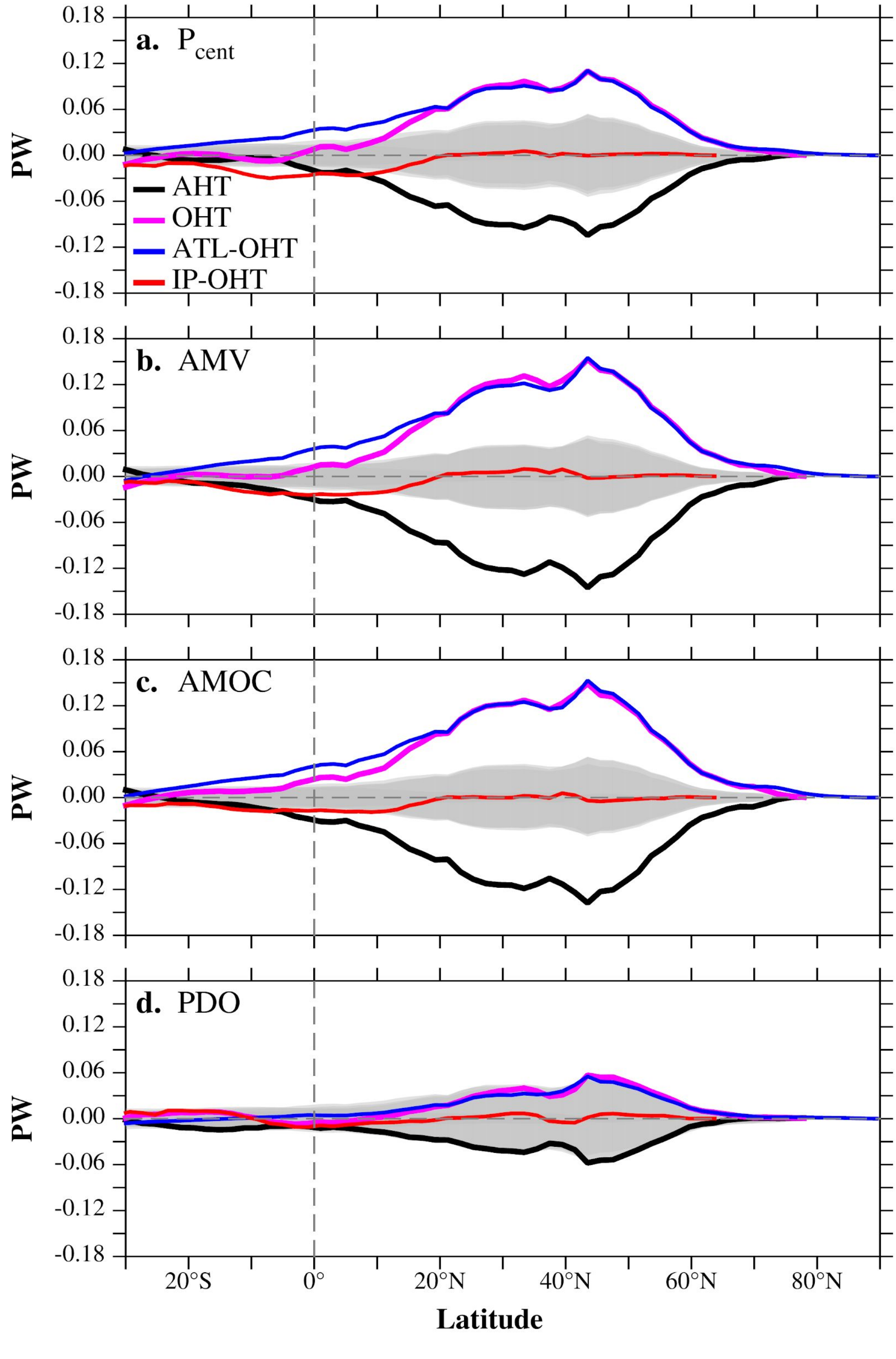

Fig. 4: As in Fig. 2 but for anomalies in the heat transport (in PW) in the atmosphere (AHT; black line), the global ocean (OHT; pink) north of 30°S, the Atlantic Ocean (ATL-OHT; blue), and the Indo-Pacific oceans (IP-OHT; red). Anomalies are calculated with the AMOC in phase, and the Pcent, the AMV, and the PDO lagging behind by 8, 3, and 10 years respectively. Gray shading masks anomalies that are non-significant at the 5% level.

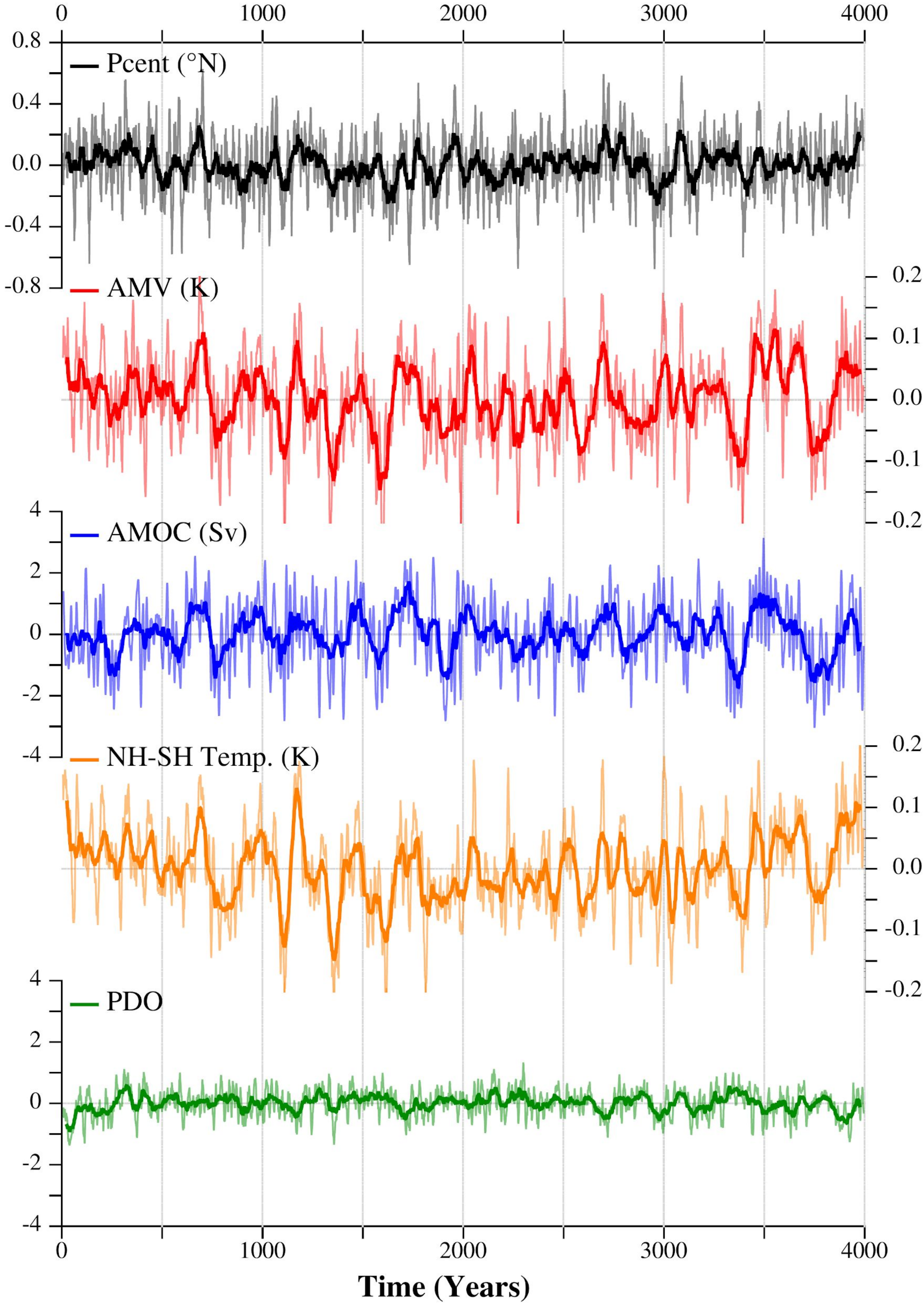

Fig. 5: Time series in the 4000-year control as in Fig. 1. Thin and thick lines are the 11- and the 51-year running means respectively.

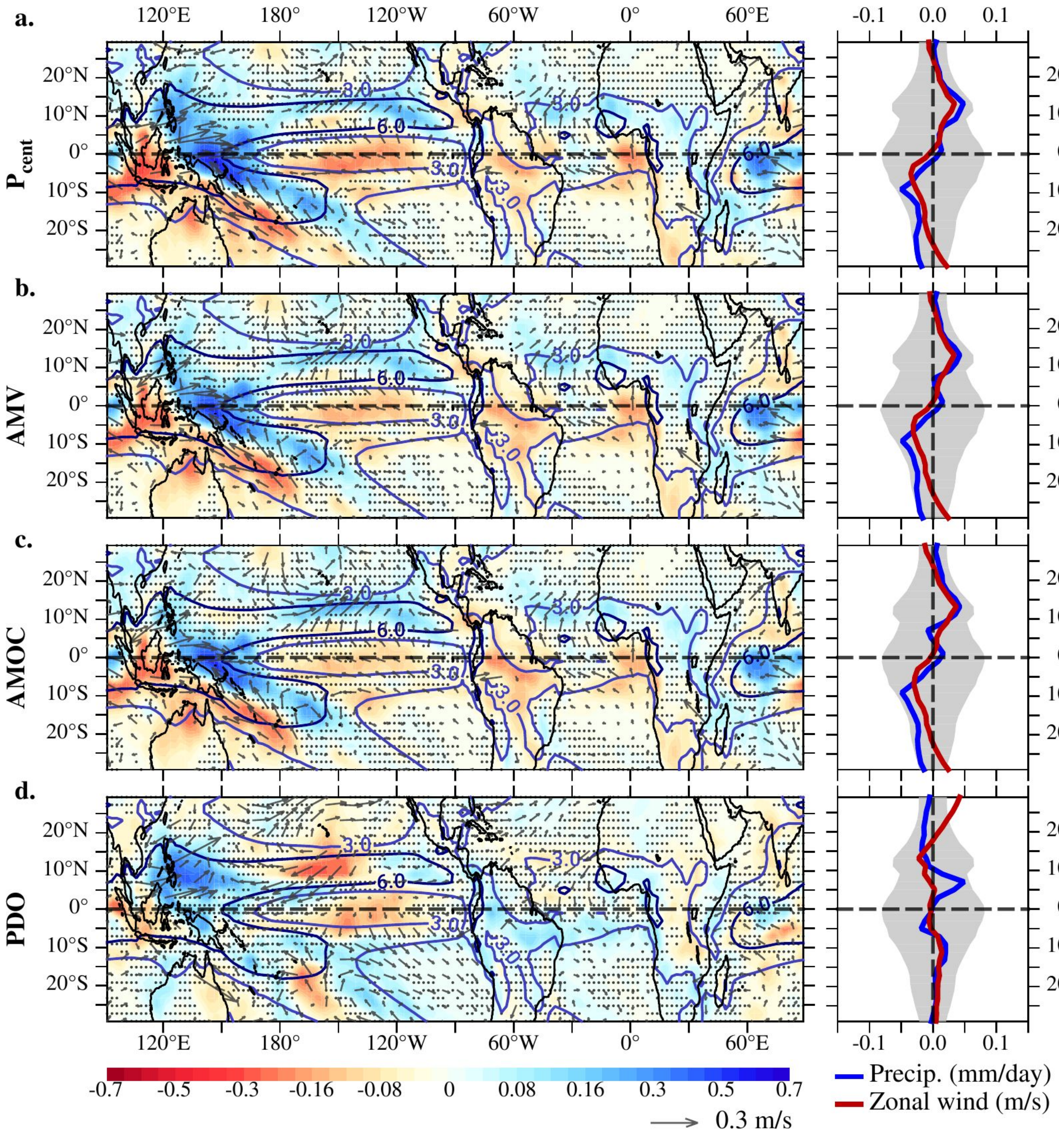

Fig. 6: As in Fig. 2 but for the band-passed indices in the 4000-year control (see text for details; indices shown in Supp. Fig. 5). Calculations are only between years 500 and 2000, when the Pcent, the AMV, and the AMOC show coherence on centennial time scales (Supp. Figs. 3 and 4). Precipitation anomalies lag behind the AMV and the AMOC by 24 years (values derived from the cross-correlation profiles in Supp. Fig. 6). No lead or lag is applied to the PDO.

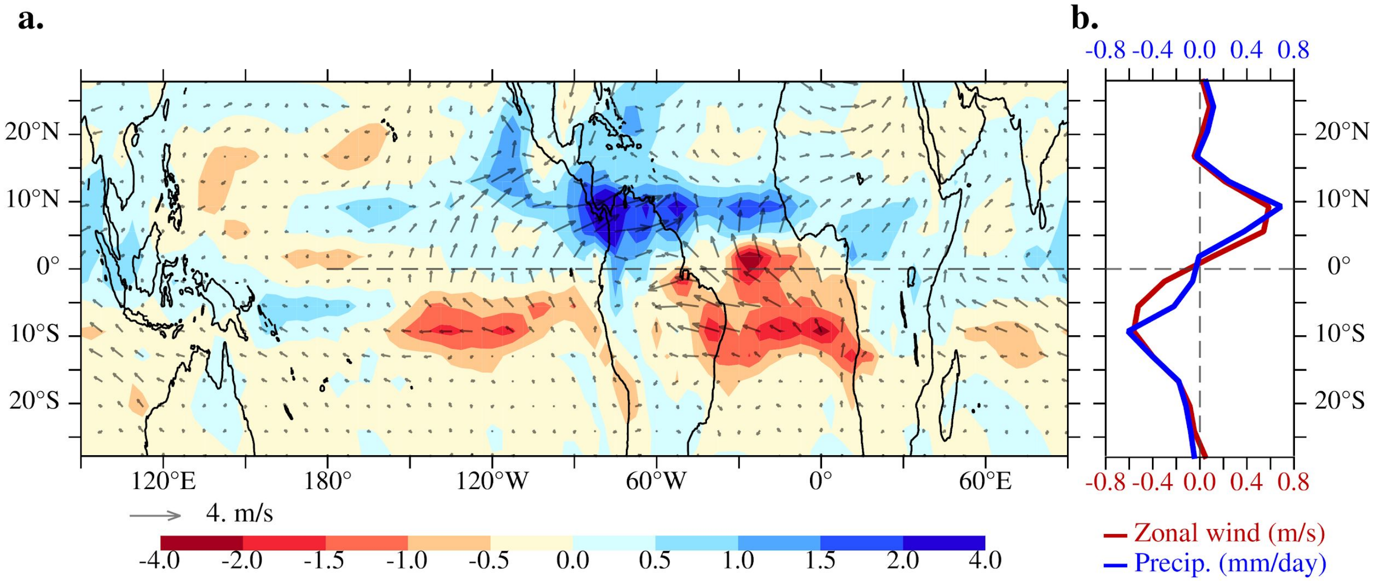

Fig. 7: **(a)** Anomalies in the annual-mean precipitation rate (shading; in mm/day) and near-surface (10 m) winds between the Last Glacial Maximum and the Heinrich Stadial 1 (averaged over the periods 20–21 kyrs and 15.5–16.5 kyrs respectively) in the TraCE-21ka simulation. Anomalies are computed to illustrate that the ITCZ is farther north during the LGM than during the HS1 and, thus, for a better comparison with Figs. 2 and 6. Note that the shading color scale of the ocean temperature is adapted for a better view of the values in the range ±2 K. No significances are shown since almost of the anomalies are statistically significant at the 5 % level (for a two-tailed Student's t test in which effective degrees of freedoms and serial autocorrelation are taken into account). **(b)** Zonally averaged anomalies in the precipitation rate (blue) and wind (red) from **(a)**. Adapted from McGee et al. [2018].